ISTITUTO NAZIONALE DI RICERCA METROLOGICA
Repository Istituzionale

The Earth's magnetic field in Italy during the Neolithic period: New data from the Early Neolithic site of Portonovo (Marche, Italy)

(Article begins on next page)

20 April 2024

1   **The Earth's magnetic field in Italy during the Neolithic period: New**

2   **data from the Early Neolithic site of Portonovo (Marche, Italy*)***

3

4   Evdokia Tema[a,b, *], Enzo Ferrara[c], Pierre Camps[d], Cecilia Conati Barbaro[e], Simone

5   Spatafora[c], Claire Carvallo[f], Thierry Poidras[d]

6

7   *[a]Dipartimento di Scienze della Terra, Università degli Studi di Torino, via Valperga 35, 10125, Torino,*

8   *Italy, evdokia.tema@unito.it*

9   *[b]ALP-Alpine Laboratory of Palaeomagnetism, via G.U. Luigi Massa 6, 12016, Peveragno, Italy*

10   *[c]Istituto Nazionale di Ricerca Metrologica, Strada delle Cacce 91, I-10135 Torino, Italy,*

11   *e.ferrara@inrim.it, simone.spatafora@edu.unito.it*

12   *[d]Géosciences Montpellier, CNRS and Université Montpellier, Montpellier, France,*

13   *pierre.camps@umontpellier.fr, poidras@gm.univ-montp2.fr*

14   *[e]Dipartimento di Scienze dell'Antichità, Sapienza Università di Roma, Roma, Italy,*

15   *cecilia.conati@uniroma1.it*

16   *[f]Institut de Minéralogie, de Physique des Matériaux et de Cosmochimie (IMPMC), Sorbonne*

17   *Universités, Paris, France, Claire.Carvallo@impmc.upmc.fr*

18

19   ** Corresponding author: Tel. +39 011 6708395, Fax. +39 011 6708398*

20

21   **ABSTRACT**

22   We present new, full geomagnetic field vector results from three Neolithic

23   ovens discovered at the archaeological site of Portonovo (Marche, Italy). The

24   discovered structures are a rare example of very well preserved underground ovens

25   from the Early Neolithic period. Standard thermal demagnetization procedures were

26   used to isolate the direction of the Characteristic Remanent Magnetization acquired

27   by the baked clay during the ovens' last firing. The corresponding archaeointensities

28   were determined by the multi-specimen procedure (MSP-DSC) and show a clear

29   intensity low during the Neolithic period. Both directional and intensity results are of

30   high quality, offering the first contribution of full geomagnetic field vector data for

31   this period in Italy. The new data are compared with other contemporaneous data

32   from Europe and with global geomagnetic field models. Independent archaeomagnetic

33   dating of the three ovens was also performed by means of the SCHA.DIF.14k model.

34   The obtained results are in excellent agreement with available radiocarbon dates and

35   confirm that all ovens belong to the Neolithic. These new data importantly enrich our

36   knowledge of the geomagnetic field during the Neolithic period that is poorly

37   documented by data, not only in Italy but also in the whole of Europe and show that

38   archaeomagnetic dating can provide precise results even for prehistoric periods.

39

41

42   1. Introduction

43   Archaeomagnetic data from ancient baked clay archaeological structures is a

44   precious source of information about the past variations of the Earth's magnetic field.

45   Thanks to archaeomagnetic records from well dated archaeological artefacts, it is

46   possible to model the variations of the geomagnetic field in the past and better

47   understand its past behaviour. Up to now, local Secular Variation (SV) curves have

48   been established for several countries, mainly in Europe, and different geomagnetic

49   field models have been proposed based on the available archaeomagnetic data at

50   regional and global level. However, most of the proposed SV curves cover only the

51   last three millennia, while the geomagnetic field variations in earlier times are still

52   poorly described.

53   In Italy, Tema et al. (2006) have published a preliminary SV curve based on

54   65 directional results ranging in time from 1300 BC to 1700AD. More recently, Tema

55   (2011) compiled an updated dataset of Italian archaeomagnetic data, presenting 73

56   directional and 23 intensity determinations. From these data, only six directional

57   results come from material older than 1000 BC. This significant lack of data from

58   periods previous to the first millennium BC can be attributed to several factors,

59   including the very limited number of well preserved still *in situ* baked clay structures

60   (often due to the use of poor building materials in prehistoric times) and the difficulty

61   of precise independent dating of such old and badly preserved structures.

62   In this study, we present new, full geomagnetic field archaeomagnetic results

63   from three Neolithic ovens excavated at the archaeological site of Portonovo (Marche,

64   Italy). The discovered ovens are a rare example of very well preserved underground

65   ovens and have the advantage of being from a well dated archaeological context with

66   three radiocarbon dates. The new results are the first full geomagnetic field vector

67   data available for this period in Italy and importantly enrich our knowledge about the

68   geomagnetic field during the Neolithic period.

69

70   **2. Archaeological site and sampling**

71   The archaeological site of Portonovo Fosso Fontanaccia (43.56º N, 13. 57 °E),

72   is situated on the Conero promontory, along the Adriatic coast of Marche (Ancona,

73   Italy). It is located on a south-facing slope, along the right bank of the river

74   Fontanaccia. It was first identified in the 1990s; since then, several excavation

75   campaigns brought into light a total of 22 underground ovens, at different heights

76   along the hillside (Fig. 1). The ovens were built by digging small cavities into the

77   colluvial layer. Almost all of them overlook large depressions in front of their

78   openings. Six of the ovens were found totally intact (Conati Barbaro, 2013). Despite

79   their different states of preservation, all ovens share similar features and dimensions:

80   the base is circular, flat, with a slight central depression, made of yellow-reddish

81   smoothed clay lining, and measuring from 1.8 to 2.0 meters in diameter; the vaults are

82   very low, so that the maximum height in the six ovens found intact does not exceed

83   50 cm; the mouths are between 60 and 80 cm in width. The inner surfaces were

84   partially coated with clay and subsequently consolidated by the firing.

85   Information about the maximum firing temperatures reached during the use of

86   the Portonovo ovens was provided by X-ray powder diffraction analysis (PXRD),

87   based on the transformation of CaO-rich sediments, structurally modified by exposure

88   to low or high temperatures clay (Muntoni and Ruggiero, 2013). PXRD analysis

89   performed on 12 samples from the hardened baked clay of the ovens inner walls

90   revealed the predominance of calcite, a variable amount of quartz and a small

91   quantity of feldspars in all samples. It also revealed the absence of Ca-silicates newly

92   formed by exposure to high temperatures, such as diopsidic pyroxenes or gehlenite,

93   typical of CaO-rich clay (Muntoni and Ruggiero, 2013). These results suggest that the

94   sediments were heated at temperatures not higher than 500 °C (Muntoni and

95   Ruggiero, 2013). Based on these relative low heating conditions, the use of the ovens

96   for pottery production may be excluded, as in that case higher heating temperatures

97   would be expected. The presence of charred cereal grains, mainly barley, within

98   ovens 14, 15 and 16, leads to the hypothesis that they were used for food processing

99   and cooking, as well as for other purposes, such as heating flint. In fact, many blades

100   and bladelets found inside and outside the ovens show clear signs of thermal

101   treatment (Conati Barbaro, 2013). Moreover, two ovens contained three adult burials

102   (two in oven 1 and one in oven 5). The secondary use of domestic structures as

103 burials, which is quite a common funerary practice during the Neolithic, probably

104 occurred when the structure itself, or perhaps the entire area, lost their primary

105 function.

106   According to the archaeological evidence, the ovens were used in the same

107 time period but most likely not all of them at the same moment. Each oven was

108 probably constructed, used for few years and then abandoned, as there is no evidence

109 of maintenance to extend its functional life. After abandonment of one oven, another

110 one was made just next to the damaged one. Based on the decoration style of some

111 pottery found, the site could be linked to the middle-Adriatic *facies* of the Italian

112 ancient Neolithic (Conati Barbaro, 2013). The homogeneity of the materials and the

113 stratigraphic data also indicate that the site was occupied for a short period of time.

114 Dating obtained from radiocarbon analysis also supports this hypothesis. Three

115 radiocarbon dates have been obtained so far (Conati Barbaro, 2013), all of them

116 carried out at CEDAD (Centro di Datazione e Diagnostica) of the University of

117 Salento, Italy, using the Accelerator Mass Spectrometry (AMS) technique.

118 Radiocarbon results were calibrated using the OxCal 3.1 software after comparison

119 with the atmospheric data reference curves (Reimer at al., 2004; 2009) and calibrated

120 ages were calculated at 95% of probability. The oldest date, carried out on a barley

121 caryopsis found inside the oven 14, suggests a calibrated age 5620-5460 BC

122 (uncalibrated age 6555 ± 45 BP, Lab code: LTL12777A). The other two dates come

123 from findings inside the oven 5; one from charcoal collected from the floor of the

124 oven dated at 5560-5350 BC (uncalibrated age 6500 ± 50 BP, Lab code: LTL5192A),

125 and the other from a bone of the male burial dated at 5480-5310 BC (uncalibrated age

126 6418 ± 50 BP, Lab code: LTL5191A). Even though it is not possible to precisely date

127 the time of use and abandonment of each oven, it is however certain that all of them

128 belong to the Early Neolithic period and they have been used between 5620-5310 BC.

129   For the archaeomagnetic study presented here, baked clay samples from the

130 ovens 14 (PFO-14), 16 (PFO-16) and 17 (PFO-17) have been collected (Fig. 1).

131 These ovens were excavated in 2013 and archaeomagnetic sampling was carried out

132 in October 2013. All of the studied ovens were found intact, with their walls and

133 vaults almost entirely preserved. Ovens PFO-14 and PFO-16 overlooked a large

134 shallow pit. Unlike these, oven PFO-17 has a trapezoidal shape and was originally

135 excavated on the edge of another pit. Ovens PFO-14 and PFO-16 were filled with

136 organic sediment containing dozens of charred cereal grains. Archaeological findings,

137 such as pottery and lithic artifacts, were rare within all the studied structures.

138   Initially, archaeomagnetic sampling was attempted with a portable rock drill.

139 However, even though the baked clay that constituted the floor and the walls of the

140 ovens was apparently compact, it proved to be extremely friable when drilled. Most

141 of the drilled cores broke in small pieces when extracting them from the oven and

142 thus they were only used for magnetic mineralogy analysis and archaeointensity

143 determinations. Systematic sampling was therefore performed with non-magnetic

144 cylindrical plastic boxes of standard dimensions (diameter= 25 mm, height= 20 mm).

145 A total of 38 samples were collected from the floor of the three ovens (15 samples

146 from oven PFO-14, 11 from oven PFO-16 and 12 from oven PFO-17). All of them

147 were independently oriented *in situ* with a magnetic compass and an inclinometer.

148

149 **3. Rock magnetic experiments**

150   Detailed magnetic mineralogy experiments on representative samples from the

151 three ovens have been performed in order to better understand the nature, the type, the

152 size and the thermal stability of magnetic minerals included in the collected baked

153 clays.

154

155   *3.1 Viscosity index*

156 In order to investigate the stability of the magnetization carried by the studied

157 samples, the viscosity index v (%) (Thellier and Thellier, 1944; Prévot, 1981) has

158 been calculated for the whole sample collection. The remanent magnetization was

159 first measured after a 15-days storage of the samples with their positive cylindrical

160 axis oriented parallel to the laboratory ambient field. Next, the remanent

161 magnetization was measured again after subsequent 15 days storage in zero field

162 (shielded chamber). The viscosity index was then calculated as the vector difference

163 between the two measurements. It was used as a quantitative estimate of the ratio of

164 the Viscous Remanent Magnetization (VRM) acquired *in situ* until the sampling, to

165 the primary remanent magnetization acquired during the last use of the ovens. For the

166 majority of the samples, the viscosity index varies from 5% to 15 % and only for four

167 samples from PFO-14 oven it is as high as 20 % (Fig. 2a). In order to guarantee that a

168 possible VRM does not importantly affect our results, we have further stored all

169 samples in zero field for 30 days before beginning the measurements.

170

171   *3.2 Isothermal remanent magnetization curves*

172 Isothermal remanent magnetization (IRM) curves have been obtained for nine

173 samples (three from each oven) at the ALP Palaeomagnetic laboratory (Peveragno,

174 Italy). An ASC pulse magnetizer was used to impart the IRM, applying stepwise

175 increasing magnetic fields up to 1.6 T, and the remanent magnetization was measured

176 with a JR6 spinner magnetometer (AGICO). The normalized IRM acquisition curves

177 obtained from the different samples are very similar and show that in most cases

178 saturation is reached at applied fields of 0.2-0.4 T (Fig. 2b). These results suggest the

179 presence of a low coercivity mineral as the main carrier of magnetization, most

180 probably magnetite.

181

182 *3.3 Thermal demagnetization of a three-axes IRM*

183 An IRM was imparted with an ASC pulse magnetizer along three orthogonal axes of

184 representative samples, applying first a maximum 1.6 T, then a medium 0.5 T and

185 finally a minimum 0.1 T magnetic field. Stepwise thermal demagnetization of this

186 composite IRM was performed to obtain unblocking temperatures of hard-, medium-

187 and soft-magnetic components (Lowrie, 1990). The demagnetization curves obtained

188 show that in all samples, most of the magnetization is carried by the magnetically soft

189 fraction (< 0.1 T) while the medium and high-coercivity components are generally

190 very small (Fig. 2c). All samples are completely demagnetized at temperatures around

191 540-560 °C while in some cases a drop of magnetization is noticed at temperatures

192 around 280 °C. These data confirm the dominance of a low coercivity mineral, most

193 probably magnetite, while some magnetic phase with low Curie temperature may be

194 also present.

195

196 *3.4 Magnetic susceptibility versus temperature (k-T) curves*

197 Low-field magnetic susceptibility versus temperature experiments (k–T curves) are

198 useful to determine the Curie temperature (T_C) and evaluate the stability of the

199 magnetic carriers upon heating. Thermomagnetic k-T curves have been performed at

200 the University of Montpellier, France. First, a piece of baked clay was crushed in an

201 agate mortar and sieved to collect the 0.4-0.8 mm size fraction. Then k–T curves were

202 acquired at low-temperature by means of a cryostat apparatus (CS-L) and at high-

203 temperature under Argon by means of a furnace (CS-3) coupled to the KLY-3

204 Kappabridge instrument (AGICO, Czech Republic). The studied material was first

205 heated from the liquid nitrogen temperature (-194 $^{\circ}$C) to about 650 $^{\circ}$C and cooled

206 down to room temperature. The data were corrected for the empty holder and

207 normalized to the maximum susceptibility. The heating-cooling curves obtained are

208 generally reversible, indicating only minor magnetic mineralogical transformations

209 during heating (Fig. 3). The Curie temperature is estimated to be around 580 $^{\circ}$C

210 suggesting the presence of magnetite, which is in agreement with our previous

211 experiments. Furthermore, these results show that the studied material is thermally

212 stable and suitable for archaeointensity study.

213

214 *3.5 Hysteresis curves*

215 Hysteresis loops and magnetic moment versus temperature profiles from

216 representative samples were measured at INRIM (Torino, Italy) with a *Lake Shore*

217 7400 Vibrating Sample Magnetometer (VSM) equipped with a thermo-resistance

218 oven operating in Ar atmosphere. The parameters obtained from the hysteresis curves

219 are plotted in a Day plot (Day et al., 1977) in order to investigate the domain state of

220 the magnetic grains (Fig. 4a). All of the studied samples fall in the pseudo single

221 domain range, indicating the presence of a mixture of SD and MD or SD and SP

222 grains (Dunlop and Carter-Stiglitz, 2006). Further investigation of the grain size was

223 following performed with FORC diagrams.

224 Thermomagnetic curves of saturation magnetization M_S versus temperature

225 (M_S-T) were also performed for representative samples. Small sample chips of about

226 50 mg were prepared, and for the same sample M_S-T curves were repeated at

227 increasing maximum temperatures. Each sample was gradually heated at 430 °C and

228 cooled back to room temperature by thermal inertia, while its magnetization was

229 continuously measured during both heating and cooling. Then, for the same sample,

230 the heating-cooling circle was repeated up to 540 °C, and finally up to 650 °C (Fig.

231 4b). Hysteresis loops have also been measured before and after thermal treatments

232 applying a maximum intensity field, H_{max}, equal to 1 T (Fig. 4c).

233   The thermomagnetic curves obtained can offer information about the magnetic

234 mineralogy, thermal stability and grain size of the magnetic carriers but also give

235 evidence about the firing temperatures achieved within the ovens during their use in

236 ancient times. Indeed, reversible changes of magnetic properties should be expected

237 when samples are experimentally heated at temperatures lower (or equal) to those

238 experienced in the past, e.g. during their use at Neolithic times (Hrouda et al., 2003;

239 Carrancho and Villalain, 2011; Spassov and Hus, 2006) while significant differences

240 are expected at higher temperatures. The results obtained show the prevalence of a

241 soft magnetic phase, with Curie (T_C) temperature below 580 °C (Fig. 4b), in good

242 agreement with the results obtained from the IRM, Lowrie experiments and k-T

243 curves. Using the derivative function of heating curves during thermomagnetic

244 analysis, T_C values have been identified between 573 °C and 577 °C, with an average

245 temperature corresponding to 575 ± 2 °C, i.e. near to the Curie point of magnetite. A

246 further confirmation of the dominance of a soft magnetic phase is given by the

247 hysteresis loops that show that the magnetization is almost completely saturated at

248 fields of around 0.3 T (Fig. 4c).

249   Comparison of the thermomagnetic curves obtained at different temperatures

250 shows that the studied material has an almost reversible behavior up to 430 °C.

251 However, when the sample is heated at higher temperatures (e.g. 540 °C and 650 °C),

252 the heating and cooling curves show an irreversible behavior, indicating that probably

253 mineralogical changes took place during heating (Fig. 4b, c). This is also confirmed

254 by the hysteresis curves that show a clear increase of the coercive force after heating

255 at 650 °C compared with the coercive force obtained before heating (Fig. 4c). Such

256 increase is probably caused by mineralogical transformations that have produced a

257 higher coercivity mineral, most probably hematite. The results obtained here suggest

258 that the firing temperatures of the ovens in ancient times were between 430 °C and

259 540 °C, in good agreement with the temperatures estimated by the X-ray powder

260 diffraction analysis (Muntoni and Ruggiero, 2013).

261

262   *3.6 First order reversal curves (FORC diagrams)*

263 In order to further characterize the grain size of the samples, first-order reversal curve

264 (FORC) diagrams were measured with a magnetometer (μ-VSM) from Princeton

265 Measurements Corporation at the IPGP-IMPMC Mineral Magnetism Analytical

266 Facility. FORC diagrams were measured with an averaging time of 0.1 s and a

267 saturating field of 1 T. One hundred and fifty FORCs were used to calculate each

268 FORC diagram. They were analyzed with the VARIFORC software (Egli, 2013),

269 using a variable smoothing factor. The variable smoothing considerably reduces the

270 noise levels by applying larger smoothing factors to the background, while preserving

271 the areas along the axes with relatively small smoothing factors.

272   A total of 7 samples from the three ovens were analyzed. The two studied

273 samples from oven PFO-14 show behavior characteristic of stable single-domain

274 grains, with most of the contours closed, and moderate interactions (Fig. 5a) (Roberts

275 et al., 2000). The outermost contours diverge slightly, which could indicate the

276 presence of a small fraction of superparamagnetic (thermally unstable) grains. The

277   coercivity peak is around 20 mT and contours extend as far as 60-70 mT. The two

278   samples from oven PFO-16 are characterized by a peak close to the Hc = 0 axis and

279   very little spreading (Fig. 5b), which seems to indicate the presence of single domain

280   grains, among which some have a relaxation time close to the time of the experiment.

281   Three samples from PFO-17 oven were measured, showing two types of behavior.

282   Sample PFO-17-1 has a FORC diagram very similar to that of PFO-16 (Fig. 5c). The

283   other two samples are characterized by two peaks: one close to the Hc = 0 axis and

284   one further away on the Hc axis, centered at Hc = 13 mT (Fig. 5d), which indicates

285   the presence of stable and viscous single domain grains. The three types of FORC

286   diagrams suggest the presence of very fine grains and little interactions, making these

287   samples ideal candidates for archaeomagnetic analyses.

288

289   **4. Methods and results**

290   *4.1 Magnetic anisotropy*

291   Before the application of the magnetic cleaning, the bulk magnetic

292   susceptibility was measured for all samples. Then, the anisotropy of the magnetic

293   susceptibility (AMS) was investigated in order to examine any possible deviation of

294   the direction of the characteristic remanent magnetization (ChRM) carried by the

295   samples with respect to the direction of the geomagnetic field in the past. All

296   measurements were performed at the ALP palaeomagnetic laboratory with a KLY-3

297   Kappabridge (AGICO). The low field bulk magnetic susceptibility varies from 1.68 x

298   10^{-3} to 14.96 x 10^{-3} SI, with the higher values coming from oven PFO-17 (Table 1).

299   The degree of AMS (P_{AMS}) (Jelinek, 1981) is very low and varies between 1.002 <

300   P_{AMS} < 1.023 with mean value 1.008 for oven PFO-14, 1.007 for PFO-16 and 1.005

301   for PFO-17 (Table 1). The anisotropy results obtained here are in agreement with

302 those from previous studies on prehistoric baked clays (e.g. Kovacheva et al., 2009)

303 and confirm that the anisotropy of baked clays from ovens and fire places is

304 negligible, in contrary to the results from brick kilns or ceramics that are usually

305 highly anisotropic (Chauvin et al., 2000; Hus et al., 2002; Tema, 2009).

306

307 *4.2 Archaeomagnetic direction determination*

308 The natural remanent magnetization (NRM) of 39 samples was first measured

309 with a JR6 spinner magnetometer at the ALP palaeomagnetic laboratory (Peveragno,

310 Italy). Subsequently, all samples were demagnetized applying stepwise alternating

311 field (AF) up to 80 mT with a ASC-D 2000 equipment. The plastic boxes used for

312 sampling prevented the application of systematic thermal demagnetization

313 procedures. Almost all samples are demagnetized in relatively low AF fields, around

314 40-60 mT, confirming the presence of a low coercivity magnetic mineral.

315 Demagnetization results are illustrated in orthogonal vector components diagrams

316 (Zijderveld, 1967) and the characteristic remanent magnetization (ChRM) for each

317 sample has been easily isolated (Fig. 6a).

318 We determined the ChRM by means of principal component analysis

319 (Kirschvink, 1980), averaged the directions thus obtained by oven, and calculated the

320 statistical parameters assuming a Fisherian Distribution (Fisher, 1953). All directions

321 at sample level are reported in Table 1, together with the Maximum Angular

322 Deviation values (MAD). The directions obtained from the three ovens are very

323 similar with each other: D= 357.0º, I=60.9º, α_{95}= 2.0, k= 448 for oven PFO-14,

324 D=357.0º, I=57.7º, α_{95}= 2.4, k= 450 for oven PFO-16 and D=352.8º, I=57.9º, α_{95}=

325 2.1, k=611 for oven PFO-17 (Fig. 6b and Table 1). All mean directions are

326 characterized by small α_{95} angles of confidence and high values of precision
327 parameter k.

328

329 *4.3 Archaeomagnetic intensity determination*

330 Absolute intensity determinations of a collection of samples from the three
331 ovens were carried out at the University of Montpellier with the multispecimen
332 protocol. The multispecimen technique offers a viable alternative to the classical
333 Thellier-Thellier method of absolute palaeointensity determination, having a great
334 potential to improve and simplify the palaeointensity measurements (Biggin and
335 Poidras, 2006; Dekkers and Böhnel, 2006; Fabian and Leonhardt, 2010). The
336 experiments were performed with a prototype of a very fast-heating infrared furnace
337 developed in Montpellier (FURéMAG, patent #1256194), which has the advantage of
338 heating samples of 10-cc-standard volume very quickly and uniformly. A total of 21
339 samples, 7 from each oven, have been studied with the MSP-DSC protocol (Fabian
340 and Leonhardt 2010). Thanks to the prototype FURéMAG furnace, a precise magnetic
341 induction field, perfectly controlled in 3D with a measured precision better than 1°
342 was applied to each sample during the heating (and cooling). The heating temperature
343 for the partial thermal remanent magnetization (pTRM) acquisition was chosen to be
344 320 °C for all samples; this temperature is considered high enough to involve a
345 sufficient fraction of the TRM (at least 20 %) but sufficiently low to avoid chemical
346 alteration. In the MSP protocol, the pTRM is imparted along the NRM direction, thus
347 no anisotropy correction is necessary. Moreover, the AMS results previously
348 discussed showed that the Portonovo samples are characterized by a very weak
349 anisotropy that would not effect the pTRM direction imparted during the laboratory

350　heatings. In multispecimen protocol, cooling rate correction is also not required

351　(Fanjat, 2012).

352　　　　A set of strict criteria was adopted to select the individual MSP data and

353　screen out those of poor technical quality. The applied criteria are essentially based on

354　three considerations.

355　　1.　The fraction of unblocked NRM during the heatings must be between 20% and

356　　　　80% of the total NRM. In this interval, the fraction is large enough to be

357　　　　accurately measured and well below a total TRM.

358　　2.　The maximum angle between the NRM left after the pTRM acquisition and

359　　　　the total NRM is fixed at 10°.

360　　3.　The relative alteration error εalt (see equation 19 in Fabian and Leonhardt,

361　　　　2010) must be lower than 10%.

362　　　　For the three ovens, all the rejected samples were discarded from further

363　analysis due to a significant alteration error (greater than 10%). The regression

364　analysis remains possible for oven PFO-14 and for oven PFO-16, with 4 samples

365　selected, while it is unfortunately precluded for oven PFO-17 since only 3 samples

366　were selected. The intensity values obtained for ovens PFO-14 and PFO-16 are very

367　similar, whatever the protocol involved (DB, FC, or DSC) in the archaeointensity

368　determination (for details about the various protocols, see Fabian and Leonhardt,

369　2010) and whatever the value of alpha parameter (see Table 2 and Figure 7). As

370　recommended by Fabian and Leonhardt (2010) our preferred archaeointensity

371　estimations are those given by the MSP-DSC protocol with the alpha parameter equal

372　to 0.5, and they are 28.2 ± 1.0 µT and 26.7 ± 0.9 µT for ovens PFO-14 and PFO-16,

373　respectively. These results show very similar intensities for the two ovens suggesting

374　that they were used and abandoned in short time periods one after the other.

375

5. New data and the geomagnetic field in southern Europe during the Neolithic period

        The new archaeomagnetic data presented in this study are the first full geomagnetic field results available up to now in Italy for the Neolithic period. Tema et al. (2006) presented two directional data from baked clay hearths excavated at the Mesolithic site of Laghetti del Crestoso (Brescia, northern Italy). Nevertheless, these results were obtained based only on NRM measurements and zero field viscosity tests and they are characterized by large α_{95} confidence angles (α_{95}= 11.6º and 17.7º respectively). Even though they give some indication about the Earth's magnetic field direction in Italy during the prehistoric time, they cannot be considered reliable enough for secular variation reconstructions. More recently, Kapper et al. (2014) studied different levels of anthropogenic burnt sediments in the Riparo Gaban rock shelter (Trento, northern Italy) and obtained seven new directional results for the time period spanning from 5000 BC to 2300 BC. These results are also characterized by relatively large α_{95} angles, varying from 5º to 13.3º, probably because of the low combustion temperatures of the sediments and possible disturbances caused by bioturbation and anthropogenic factors (Kapper et al., 2014). No intensity data from Italian artifacts with ages older than the last two millennia are available before now (Tema, 2011).

        Archaeomagnetic data from the prehistoric period are also extremely scarce in the whole of central Europe. To our knowledge, only two directional data from Germany and few data from Hungary are available for the 6000-4000 BC period. Schnepp et al. (2004) presented the archaeomagnetic direction of an oven excavated at Untergaiching (southern Germany) and Schnepp and Lanos (2005) obtained one

more directional result from Germany by studying the archaeomagnetic direction of an oven excavated at Bernstorf, close to Kranzberg in southern Germany, with an age between 5526 BC and 5373 BC. Márton (2009) published a set of prehistoric archaeomagnetic directions from different sites in Hungary, with ^{14}C ages ranging from 5500 BC to 4490 BC (no age errors are reported in the publication). Regarding the archaeomagnetic intensity data, again almost no data are available, with the exception of few archaeointensity records from Czech Republic reported in the early work of Bucha (1967). Conversely, an extended dataset of both directional and intensity data is available for Eastern Europe, mainly coming from the Balkan Peninsula (Tema and Kondopoulou, 2011). Bulgaria has one of the richest archaeomagnetic records in Europe that covers almost continuously the last 8000 years (Kovacheva et al., 2009; 2014) while an important number of directional (De Marco et al., 2014) and intensity data (De Marco et al., 2008) are also available for Greece. Few data from prehistoric times are also available from other countries of Eastern Europe such as Serbia and Romania (Brown et al., 2015, Geomagia50.v3.1 database).

The new full geomagnetic field results presented here are compared with published data from Italy, central Europe and Balkan Peninsula available for the 6000-4000 BC period (Fig. 8). Data from the Balkan Peninsula (Tema and Kondopoulou, 2011) have been updated with some recently published data from Bulgaria (Kovacheva et al., 2014) and Greece (Fanjat et al., 2013), taken from the updated Geomagia50.v3.1 database. For comparison, all data have been relocated at Viterbo (42.45 ºN, 12.03 ºE), situated in central Italy (around 70 km from Rome), which was chosen as the optimum reference point for archaeomagnetic studies in Italy (Lanza and Zanella, 2003; Tema et al., 2006; 2010). The comparison shows that the

425 directions obtained from the Portonovo ovens are in very good agreement with the

426 data from Germany and Hungary from the same time period (Fig. 8a, b). Good

427 agreement can also be observed with the directional data from the Balkan Peninsula.

428 As far as the intensity data are concerned, Portonovo results clearly show a low

429 intensity value around 28±1 µT. This low intensity seems to be confirmed by some

430 data from Bulgaria that show intensity values of around 30-35 µT, even though some

431 dispersion in the published data can be noticed around 5500 BC, with intensities as

432 high as 45 µT (Fig. 8c).

433   The new data have been also compared with the predictions of the

434 CALS10k.1b (Korte et al., 2011), the pfm9k.1a (Nilson et al., 2014) and the

435 SCHA.DIF.14k (Pavon-Carrasco et al., 2014) global geomagnetic field models that

436 are the most recently published models that cover the Neolithic period. The Portonovo

437 directions are in very good agreement with the models, while the Portonovo intensity

438 is lower than the models predictions (Fig. 8). Actually, both pfm9k.1a and

439 SCHA.DIF.14k models tend to show an important decrease in intensity for the period

440 around 5500 BC. However, the model predictions show much smoother variations

441 with respect to those indicated by the archaeomagnetic data, probably influenced by

442 the sedimentary records included in the reference dataset of some models for the BC

443 periods and/or the often the important dispersion of the reference data. This clearly

444 highlights the importance of new, high quality data that can contribute to

445 improvement of the models' resolution.

446

447 **6. Discussion and conclusions**

448   The material collected from the Neolithic ovens of Portonovo, even if very

449 fragile and baked at relatively low temperatures (<500 ºC), has been shown to be a

reliable recorder of the Earth's magnetic field in the past. Both directional and intensity results obtained are of high quality, offering the first full geomagnetic field vector data for Neolithic period in Italy. The directions and intensities recorded by the three ovens are very similar, suggesting that the ovens were in use and abandoned almost at the same time or in time periods very close one to the other, when the geomagnetic field was almost the same. This is in very good agreement with the archaeological findings suggesting that each oven was in use for a very short period of time (few years or decades), while the whole site was occupied for just few centuries.

Taking into account the very well determined geomagnetic field vector, with directions accompanied by low α_{95} angles of confidence and intensities characterized by small confidence intervals, we have tried to further investigate the possibility of reconstructing the chronological sequence of the construction and abandonment of the three studied ovens by archaeomagnetic dating. We have therefore compared the declination, inclination and intensity determined for each oven with the predictions of the SCHA.DIF.14k European geomagnetic field model (Pavón-Carrasco et al., 2014), that is only based on archaeomagnetic and volcanic rock data and therefore offers one of the most reliable global geomagnetic field models for the prehistoric period. For oven PFO-17, dating was performed based only on declination and inclination. Such comparison shows that at 95 % of probability the last firing of each oven occurred at: 5479-5403 BC for oven PFO-14 (or 5463-5429 BC at 65% of probability), 5472-5395 BC for oven PFO-16 (or 5455-5423 BC at 65 % of probability) and 5522-5359 BC for oven PFO-17 (or 5503-5405 BC at 65% of probability). Dating obtained for oven PFO-17 based only on the direction shows a quite wide time interval, demonstrating that the contribution of archaeointensity is very important for restricting the archaeomagnetic dating results. Nevertheless, the dating results of all ovens are in

very good agreement with the dating of the site based on archaeological evidence and available ^{14}C dating.

Archaeomagnetic dating results suggest that the PFO-17 oven is most likely to belong to a separate group of ovens and it was damaged and abandoned before ovens PFO-14 and PFO-16. On the other hand, ovens PFO-14 and PFO-16 are most probably abandoned at the same time or with very short time difference in presence of actually almost the same ambient geomagnetic field. This hypothesis seems to be also supported by the vicinity of the two ovens, and probably when one was damaged by repeated use, the other was built just attached to the previous one. Of course this interpretation should be used with caution and integrated with other archaeological evidence, as the wide dating interval obtained for oven PFO-17 and the overlapping of the obtained archaeomagnetic dating for PFO-14 and PFO-16 ovens caused by their statistically similar directions and intensities, does not allow more precise chronological reconstruction. Moreover, archaeomagnetic dating always refers to the last firing of the ovens, usually corresponding to their abandonment but it can not offer information about the date of construction or period of use of the structures that could have occurred much earlier.

The new full geomagnetic field vector results presented here aim to offer new data about the Earth's magnetic field in Italy during the Neolithic period and enrich the available global dataset that is still poor for the prehistoric period. The clear, well defined, low intensity values obtained here suggest that the intensity of the Earth's magnetic field around 5500 BC was almost 20 µT lower that the today's field in Italy. Such low intensity seems to be an interesting feature of the field in Neolithic period, noticed also in the Balkan Peninsula, and it should be further investigated by obtaining new high quality data from Europe from the same chronological period.

500 Undoubtedly, obtaining new data from well-dated archaeological material is also a

501 key issue for improving the resolution of geomagnetic field models in the past, in

502 order to identify the fine features and rapid geomagnetic field variations, as well as

503 extending reliable archaeomagnetic dating in prehistoric periods.

504

505

514

515

516

517 **References**

518 Biggin, A.J., Poidras, T., 2006. First-order symmetry of weak-field partial

519 thermoremanence in multi-domain ferromagnetic grains. 1. Experimental evidence

520 and physical implications. Earth and Planetary Science Letters, 245(1-2), 438–453.

521 doi:10.1016/j.epsl.2006.02.035.

522

523 Brown, M.C., Donadini, F., Korte, M., Nilsson, A., Korhonen, K., Lodge, A.,

524 Lengyel, S.N., Constable, C.G., 2015. GEOMAGIA50.v3: 1. General structure and

525 modifications to the archeological and volcanic database. Earth Planets Space, 67:83,

526 doi:10.1186/s40623-015-0232-0.

527

528 Bucha, V., 1967. Intensity of the Earth magnetic field during archeological times in

529 Czechoslovachia. Archaeometry, 10, 12-22, doi: 0.1111/j.1475-4754.1967.tb00608.x.

530

531 Carrancho, A., Villalaín, J.J., 2011. Different mechanisms of magnetization recorded

532 in experimental fires: archaeomagnetic implications. Earth and Planetary Science

533 Letters, 312, 176-187.

534

535 Chauvin, A., Garcia, Y., Lanos Ph., Laubenheimer, F., 2000. Palaeointensity of the

536 geomagnetic field recovered on archaeomagnetic sites from France. Physics Earth

537 Planetary Interiors, 120, 111-136.

538

539 Conati Barbaro, C., 2013. Cooking, working and burying in Ancient Neolithic: The

540 ovens of Portonovo (Marche, Italy)), with contributions by Acquafredda P., Catalano

541   P., Celant A., Di Giannantonio S., Lelli R., Muntoni I.M., Pallara M., Ruggero G.

542   Origini, XXXV, 31-82.

543

544   Day, R., Fuller, M., Schmidt, V.A., 1977. Hysteresis properties of titanomagnetites:

545   Grain size and composition dependence. Physics Earth and Planetary Interiors, 13,

546   260-267.

547

548   De Marco, E., Spatharas, V., Gómez-Paccard, M., Chauvin, A., Kondopoulou D.,

549   2008. New archaeointensity results from archaeological sites and variation of the

550   geomagnetic field intensity for the last 7 millennia in Greece. Phys. Chem. Earth, 33,

551   578-595.

552

553   De Marco, E., Tema, E., Lanos, Ph., Kondopoulou, D., 2014. An updated catalogue of

554   Greek archaeomagnetic data for the last 4500 years and a directional secular variation

555   curve. Stud. Geophys. Geod., 58, 121-147, doi: 10.1007/s11200-013-0910-y.

556

557   Dekkers, M. J., Böhnel, H. N., 2006. Reliable absolute palaeointensities independent

558   of magnetic domain state. Earth and Planetary Science Letters, 248 (1-2), 508–517,

559   doi: 10.1016/j.epsl.2006.05.040.

560

561   Dunlop, D.J., Carteer-Stiglitz, B., 2006. Day plots of mixtures of superparamagnetic,

562   single-domain, pseudosingle-domain, and multidomain magnetites. Journal of

563   Geophysical Research, 111, B12S09, doi: 10.1029/2006JB004499.

564

565   Egli, R. 2013. VARIFORC: An optimized protocol for calculating non-regular first-

566   order reversal curve (FORC) diagrams. Global and Planetary Change, 110, 302-320.

567   http://dx.doi.org/10.1016/j.gloplacha.2013.08.003.

568

569   Fabian, K., Leonhardt R., 2010. Multiple-specimen absolute paleointensity

570   determination: an optimal protocol including pTRM normalization, domain-state

571   correction, and alteration test. Earth Planetary Science Letters, 207, 84-94.

572

573   Fanjat G., 2012. Les fluctuations du champ magnétique terrestre : des variations

574   séculaires récentes aux renversements. *Available online at https://tel.archives-*

575   *ouvertes.fr/tel-00719380.*

576

577   Fanjat, G., Aidona, E., Kondopoulou, D., Camps, P., Rathossi, C., Poidras, T., 2013.

578   Archeointensities in Greece during the Neolithic period: New insights into material

579   selection and secular variation curve. Phys. Earth Planet. Int., 215, 29-42, doi:

580   10.1016/j.pepi.2012.10.011.

581

582   Fisher R.A., 1953. Dispersion on a sphere. Proceedings of Royal Society, London,

583   pp.295.

584

585   Jelinek, V., 1981. Characterization of the magnetic fabric of rocks. Tectonophysics,

586   79, 63-67.

587

588   Hrouda, F. 2003. Indices for numerical characterization of the alteration processes of

589   magnetic minerals taking place during investigation of temperature variation of

590   magnetic susceptibility. Studia Geophysica et Geodaetica, 47, 847-861.

591

592   Hus, J., Ech-Chakrouni, S., Jordanova, D., 2002. Origin of magnetic fabric in bricks:

593   its implications in archaeomagnetism. Phys. Chem. Earth, 27, 1319-1331.

594

595   Kapper, L., Anesin, D., Donadini, F., Angelucci, D., Cavulli, F., Pedrotti, A., Hirt, A.,

596   2014. Linking site formation processes to magnetic properties. Rock- and

597   Archeomagnetic analysis of the combustion levels at Riparo Gaban, Italy. Journal of

598   Archaeological Science, 41, 836-855.

599

600   Kirschvink J.L., 1980. The least-square line and plane and the analysis of

601   palaeomagnetic data. Geophys. J. Astron. Soc., 62, 699-718.

602

603   Korte, M., Constable, C., Donadini, F., Holme, R., 2011. Reconstructing the Holocene

604   geomagnetic field. Earth Planetary Science Letters, 312, 3-4, 497-505, doi:

605   10.1016/j.epsl.2011.10.031.

606

607   Kovacheva, M., Chauvin, A., Jordanova, N., Lanos, Ph., Karloukovski, V., 2009.

608   Remanence anisotropy effect on the palaeointensity results obtained from various

609   archaeological materials, excluding pottery. Earth Planets Space, 61, 711-732.

610

611   Kovacheva, M., Kostadinova-Avramova, M., Jordanova, N., Lanos, Ph., Boyadziev,

612   Y., 2014. Extended and Revised Archaeomagnetic Database and secular variation

613   curves from Bulgaria for the Last Eight Millennia. Physics Earth and Planetary

614   Interiors, 236, 79-94.

615

616   Lanza, R., Zanella, E., 2003. Palaeomagnetic secular variation at Vulcano (Aeolian

617   Islands) during the last 135 kyr. Earth Planet. Sci. Lett., 213, 321-336.

618

619   Lowrie, W., 1990. Identification of ferromagnetic minerals in a rock by coercivity and

620   unblocking temperature properties. Geophys. Res. Lett., 17, 159-162.

621

622   Márton, P., 2009. Prehistorical archeomangetic directions from Hungary in

623   comparison with those from South-eastern Europe. Earth Planets Space, 61, 1351-

624   1356.

625

626   Muntoni, I.M., Ruggiero, G., 2013. Estimating the Firing temperatures of

627   pyrotechnological processes in Neolithic site of Portonovo. Origini, XXXV, 52-56.

628

629   Nilsson, A., Holme, R., Korte, M., Suttie, N., Hill, M., 2014. Reconstructing

630   Holocene geomagnetic field variation: new methods, models and implications.

631   Geophysical Journal International, 198, 1, 229-248.

632

633   Pavón-Carrasco, F.J., Osete, M.L., Torta, J.M., De Santis, A., 2014. A geomagnetic

634   field model for the Holocene based on archaeomagnetic and lava flow data. Earth

635   Planetary Science Letters, 388, 98 - 109.

636

637 Prévot, M., 1981. Some aspects f magnetic viscosity in subaerial and submarine

638 volcanic rocks. Geophys. J. R. Astr. Soc., 66, 169-192.

639

640 Reimer, P.J., Baillie, M.G.L.,Bard, E., Bayliss, A., Beck, J.W., Bertrand, C.,

641 Blackwell, P.G., Buck, C.E., Burr, G., Cutler, K.B., Damon, P.E., Edwards, R.L.,

642 Fairbanks, R.G., Friedrich, M., Guilderson, T.P., Hughen, K.A., Kromer, B.,

643 McCormac, F.G., Manning, S., Bronk Ramsey, C., Reimer, R.W., Remmele, S.,

644 Southon, R.J., Stuiver, M., Talamo, S., Taylor, F.W., van der Plicht, J.,

645 Weyhenmeyer, C.E., 2004. IntCal04 Terrestrial radiocarbon age calibration, 0-26 Cal

646 Kyr BP. Radiocarbon, 46 (3), 1029-1058.

647

648 Reimer, P.J., Baillie, M.G.L., Bard, E., Bayliss, A., Beck, J.W., Blackwell, P.G.,

649 Bronk Ramsey, C., Buck, C.E., Burr, G.S., Edwards, R.L., Friedrich, M., Grootes,

650 P.M., Guilderson, T.P., Hajdas, I., Heaton, T.J., Hogg, A.G., Hughen, K.A., Kaiser,

651 K.F., Kromer, B., McCormac, F.G., Manning, S.W., Reimer, R.W., Richards, D.A.,

652 Southon, J.R., Talamo, S., Turney, C.S. M., van der Plicht, J., Weyhenmeyer, C.E.

653 2009. IntCal09 and Marine09 radiocarbon age calibration curves, 0-50,000 years cal

654 BP. Radiocarbon, 51(4), 1111-1150.

655

656 Roberts, A. P., Pike, C. R. and Verosub, K. L., 2000. First order reversal curve

657 diagrams: a new tool for characterizing the magnetic properties of natural samples.

658 Journal of Geophysical Research , 105, 28461-28475.

659

660 Schnepp, E., Lanos, Ph., 2005. Archaeomagnetic secular variation in Germany during

661 the past 2500 years. Geophysical Journal International, 163, 479-490.

662

663 Schnepp, E., Pucher, R., Reinders, J., Hambach, U., Soffel, H., Hedley, I., 2004. A

664 German catalogue of archaeomagnetic data. Geophysical Journal International, 157,

665 64-78, doi: 10.1111/j.1365-246X.2004.02163.x.

666

667 Spassov, S., Hus, J., 2006. Estimating baking temperatures in a Roman pottery kiln by

668 rock magnetic properties: implications of thermochemical alteration on

669 archaeointensity determinations. Geophysical Journal International, 167, 592-604.

670

671 Tema, E., Kondopoulou, D., 2011. Secular variation of the Earth's magnetic field in

672 the Balkan region during the last eight millennia based on archaeomagnetic data.

673 Geophysical Journal International, 186, 2, 603-614, doi: 10.1111/j.1365-

674 246X.2011.05088.x

675

676 Tema, E., Goguitchaichvili, A., Camps P., 2010. Archeointensity determination from

677 Italy: new data and Earth's magnetic field strength variation over the past three

678 millennia. Geophysical Journal International, 180, 596-608, doi: 10.1111/j.1365-

679 246X.2009.04455.x

680

681 Tema, E., Hedley, I., Lanos, Ph., 2006. Archaeomagnetism in Italy: A compilation of

682 data including new results and a preliminary Italian Secular Variation curve.

683 Geophysical Journal International, 167, 1160-1171.

684

685 Tema, E., 2009. Estimate of the magnetic anisotropy effect on the archaeomagnetic

686 inclination of ancient bricks. Physics of Earth and Planetary Interiors, 176, 213-223,

687 doi: 10.1016/j.pepi.2009.05.007.

688

689 Tema, E., 2011. Archaeomagnetic Research in Italy: Recent achievements and future

690 perspectives. In: The Earth's Magnetic Interior, IAGA Special Sopron Book Series,

691 Volume 1, Chapter 15, pp. 213-233. Eds: Petrovsky, E., Herrero-Bervera, E.,

692 Harinarayana, T., Ivers, D., Springer, doi: 10.1007/978-94-007-0323-0_15.

693

694 Thellier, E., Thellier, O., 1944. Recherches géomagnetiques sur les coulees

695 volcaniques d'Auvergne. Ann. Geophys., 1, 37–52.

696

697 Zijderveld, J., 1967. AC demagnetization of rocks: analysis of results. In: Collinson,

698 D., Creer, K., Runcorn, S. (Eds.), Methods in Paleomagnetism. Elsevier, New York,

699 pp. 254-256.

700

701 **Figures captions**

702 Fig. 1. a) Map of Italy with the location of the Portonovo archaeological site; b-c)

703 General view of the excavated ovens; d) Photo of the PFO17 oven; e) General view of

704 the PFO14, PFO16 and PFO16 ovens, sampled for archaeomagnetic analysis.

705

706 Fig. 2. a) Histograms of the viscosity index (%) calculated for the three ovens; b)

707 Normalized IRM acquisition curves up to 1.6 T for representative samples from the

708 three ovens; c) Stepwise thermal demagnetization of three IRM components following

709 Lowrie (1990). Symbols: dot= Soft- (0.1 T); diamond= Medium- (0.5 T); square=

710 Hard- (1.6 T) coercivity component.

711

712 Fig. 3. Low-field susceptibility versus temperature curves measured under air

713 atmosphere (k-T curves) for a representative sample from oven PFO17. Susceptibility

714 values are normalized to the maximum susceptibility. The heating curve is in red, the

715 cooling curve is in blue.

716

717 Fig. 4. a) Day plot obtained from the hysteresis curves of representative specimens

718 from the three ovens. The SD-MD and SD-SP mixing lines are calculations for

719 magnetite from Dunlop and Carter-Stiglitz (2006). Numbers along curves are volume

720 fractions of the soft component (SP or MD) in mixtures with SD grains. All the data

721 plot on the PSD range; b) Thermomagnetic profiles (M-T) obtained for the PFO17a

722 sample after subsequent heating from room temperature up to 430 °C (left), 540 °C

723 (middle), and 650 °C (right). All heating-cooling curves have been normalized to the

724 initial magnetization at room temperature, before any treatment; c) Hysteresis curves

725 obtained for the same PFO17a sample, before (black line) and after treatment at 430

726   °C (red), 540 °C (green) and 650 °C (blue). The inset shows the behavior of the cycles

727   around the origin of the graphs.

728

729   Fig. 5. FORC diagrams obtained from samples a) PFO14-1; b) PFO16-1; c) PFO17-1

730   and d) PFO17-3. Each FORC diagram is calculated from 150 FORCs measured with

731   an averaging time of 0.1s. Note that the horizontal and vertical scales are the same for

732   the four diagrams.

733

734   Fig. 6a.) Stepwise thermal demagnetization results from representative samples from

735   the PFO-14 (left), PFO-16 (middle) and PFO-17 (left) ovens illustrated as Zijderveld

736   plots. Symbols: full dots = declination; open dots = apparent inclination; b) Equal area

737   projections of the ChRM directions at sample level for the three ovens. The big dot

738   represents the mean value calculated for each oven according to Fisher statistics.

739

740   Fig. 7. Multi-specimen (MSP) archaeointensity determinations for a) and b) oven

741   PFO14 and c) and d) oven PFO16. Closed (open) symbols represent data used

742   (rejected) in the robust regression of the responses in Q parameters on the predictors

743   in magnetic field B. The MSP-BD and MSP-FC data and fitting lines are represented

744   with magenta and blue lines, respectively. For MSP-DSC plots (red lines), data and

745   fitting lines are calculated with $\alpha = 0.5$. The dashed lines are the 65% confidence

746   intervals on the best fitting lines.

747

748   Fig. 8. The new declination (top), inclination (middle) and intensity (bottom) data

749   obtained in this study plotted together with available literature data from Italy, central

750   Europe and Balkan Peninsula for the 6000-4000 BC period. The SV curves calculated

751   from the pfm9k.1a, CALS10K.1b and SCHA.DIF.14k global geomagnetic field

752   models have been also plotted for comparison.

753

754

755 **Tables**

756 Table 1. Archaeomagnetic results. Columns: Sample; Natural Remanent

757 Magnetization; Bulk susceptibility; $P_{AMS:}$ degree of the Anisotropy of Magnetic

758 Susceptibility; Declination (º); Inclination (º); MAD: Maximum Angular Deviation;

759 Mean direction: N= number of independently oriented samples; D_m= mean

760 declination; I_m= mean inclination; α_{95}= 95% semi-angle of confidence; k= precision

761 parameter according to Fisher (1953).

762

763 Table 2. Archaeointensity results for ovens PFO-14, PFO-16 and PFO-17.

764 MSP archaeointensity values are estimated by the zero-crossing point of the Robust

765 linear regression on the Q parameters obtained with the MSP-DB protocol (Dekker

766 and Bohnel, 2006), fraction correction (MSP-FC) or domain state correction protocols

767 (Fabian and Leonhardt, 2010) as function of the laboratory field. R-squared is the

768 coefficient of determination indicating how well data fit the model. RMSE is the root

769 mean squared error for the fitting line.
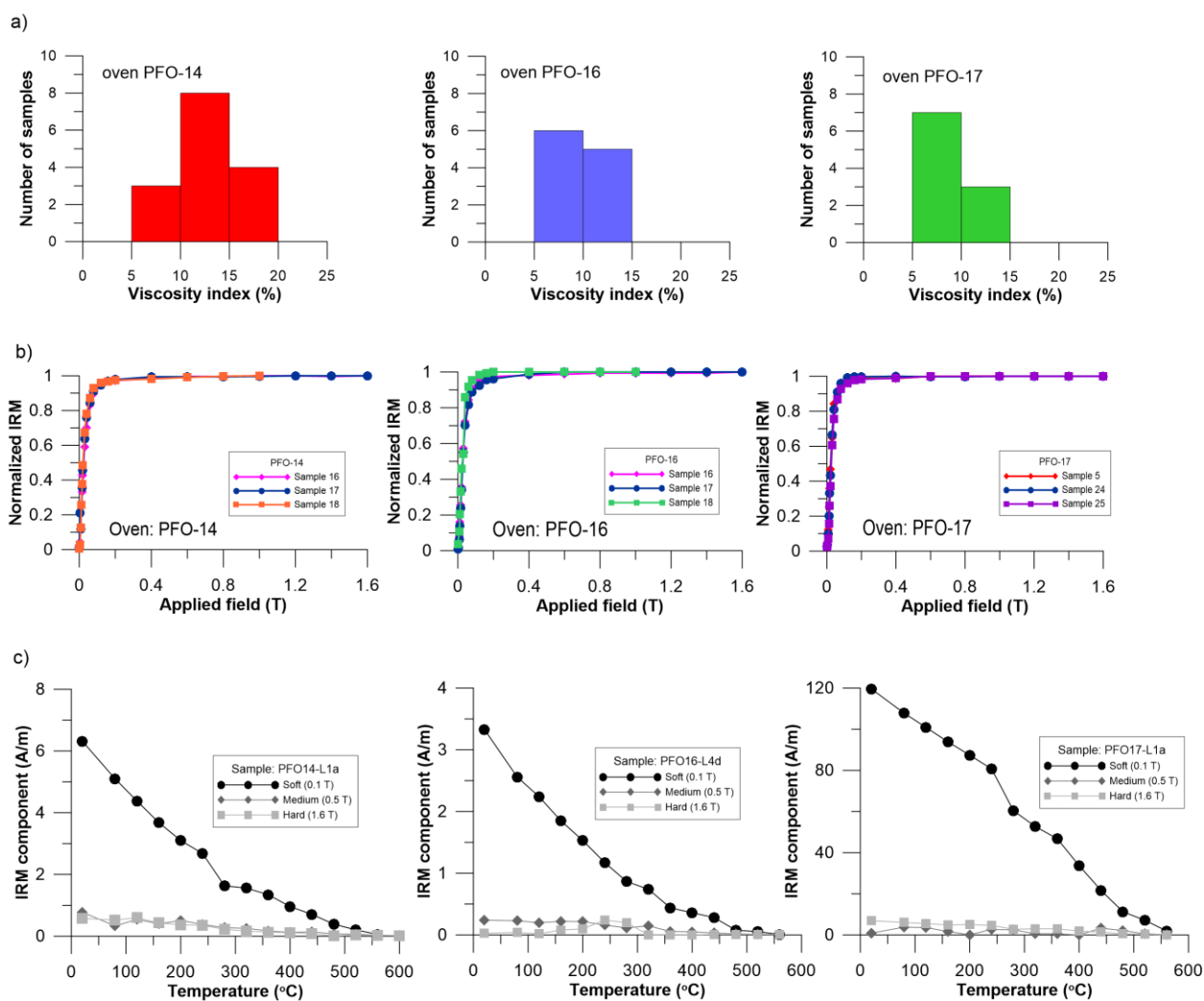
770
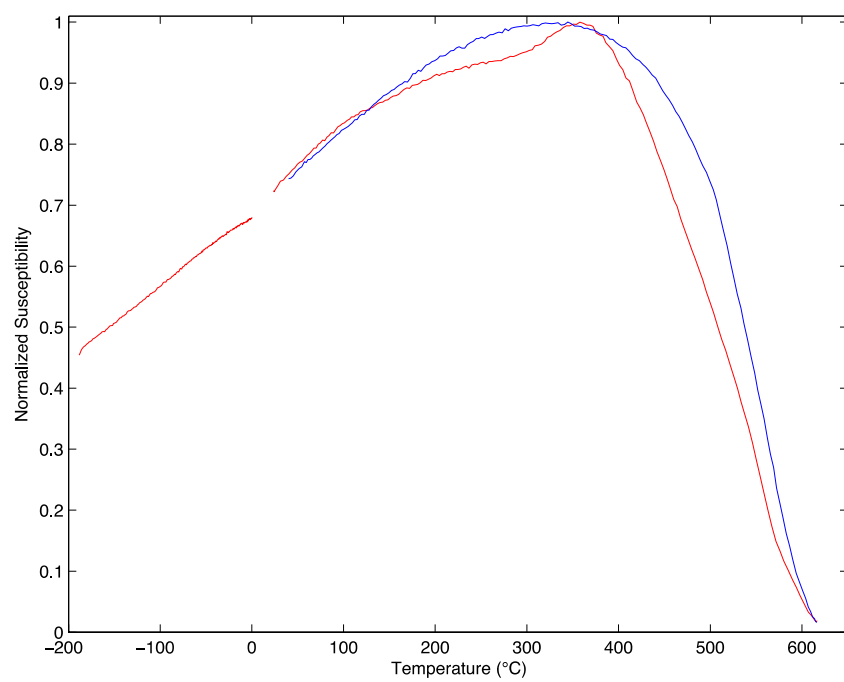
771

772

773
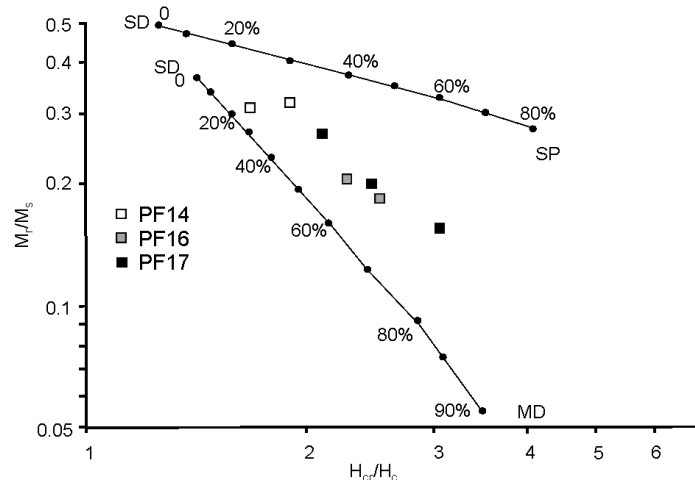
774

Fig. 1

776

777

778

779

780

781

782

783

784

Fig. 2

787

788

789

790

791

792

793

794

795

Fig. 3

796

797

798

799

800

(a)

801

802

803

Normalized M

804

805

806

up 430 °C

down 430 °C

PFO 17a

T$_{max}$ = 430 °C

T (°C)

up 540 °C

down 540 °C

PFO 17a

T$_{max}$ = 540 °C

T (°C)

PFO 17a

T$_{max}$ = 650 °C

up 650 °C

down 650 °C

T (°C)

807

(b)

808

809

(c)

810

Fig. 4

PFO 17a

430 °C

25 °C

540 °C

650 °C

M (Am^{2}kg^{-1})

Applied Field (T)

PFO 17a

650 °C

25 °C

430 °C

540 °C

SD

0

20%

40%

60%

80%

SP

SD

0

20%

40%

60%

80%

90%

MD

M$_r$/M$_s$

H$_{cr}$/H$_c$

PF14

PF16

PF17

811

812

a) PFO14-1

b) PFO16-1

c) PFO17-1

d) PFO17-3

813

814

Fig. 5

816

817

818

(a)

819

820

821

(b)

822

823

Fig. 6

824
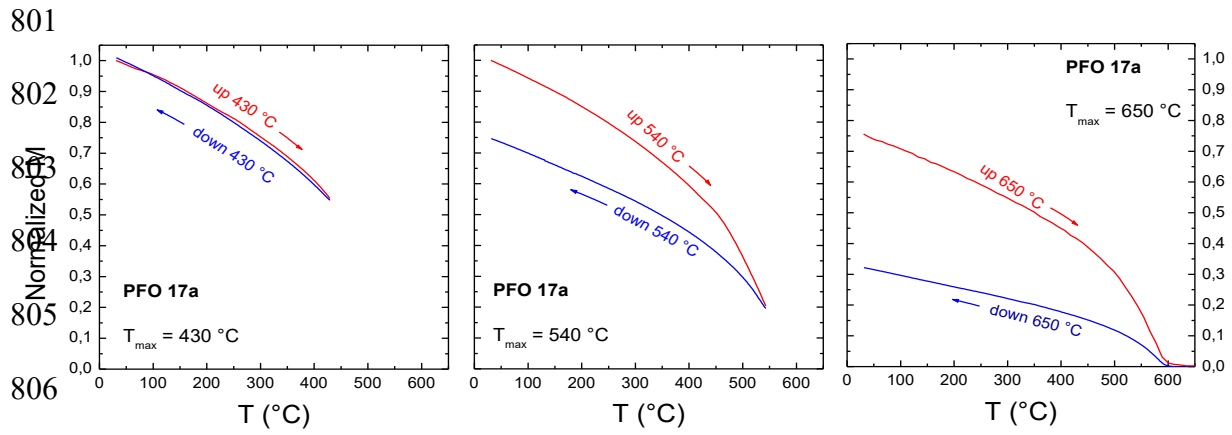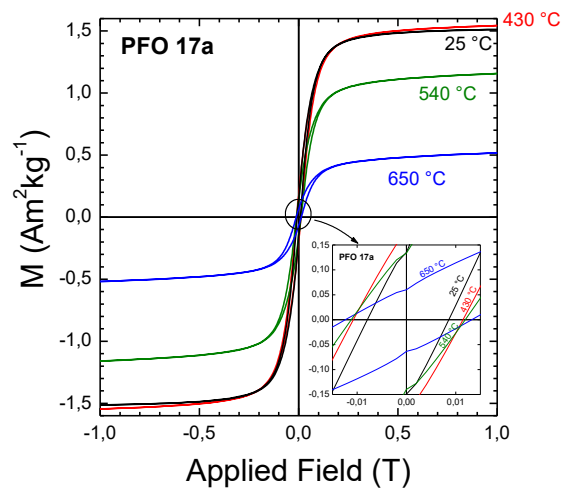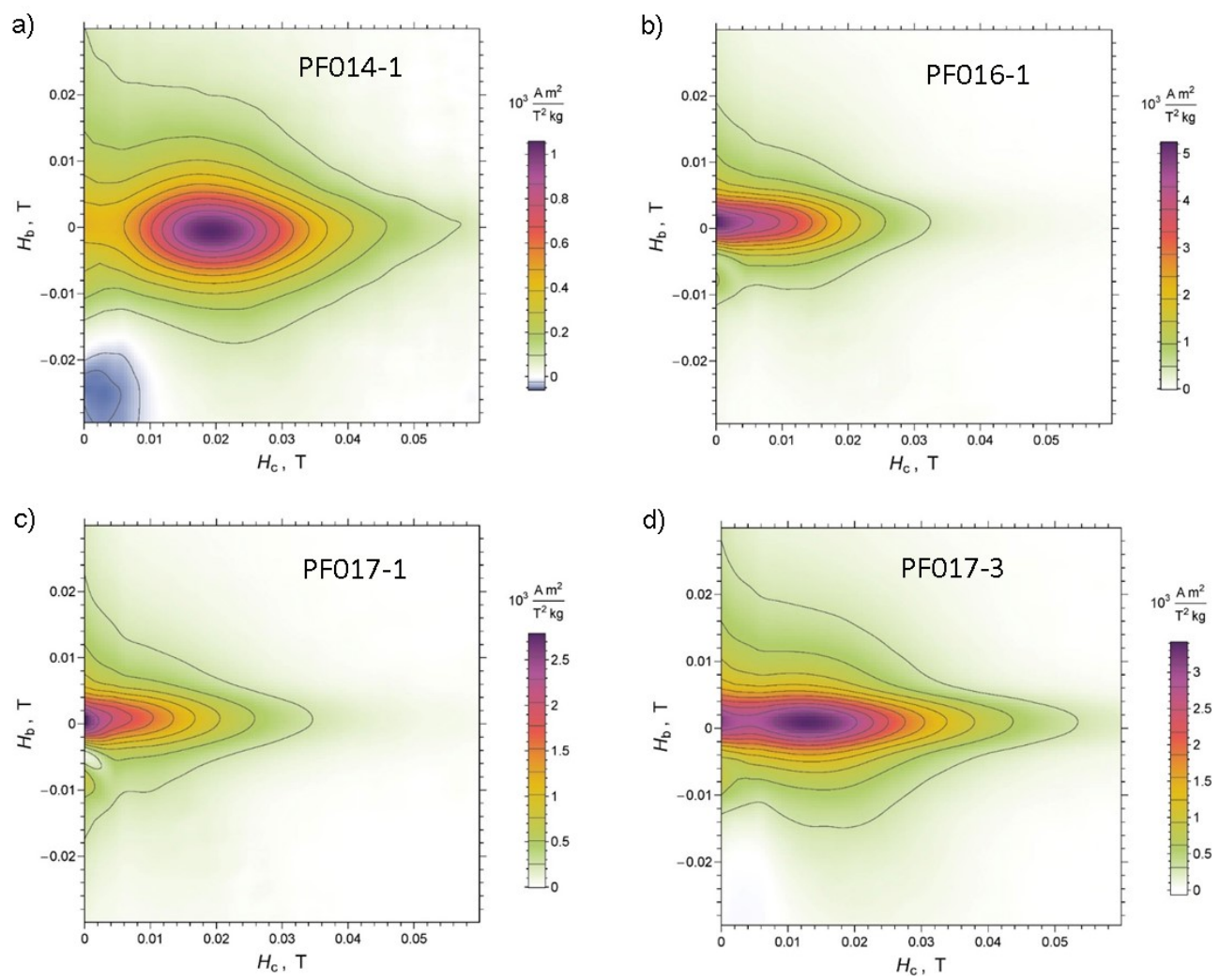
825

826

827
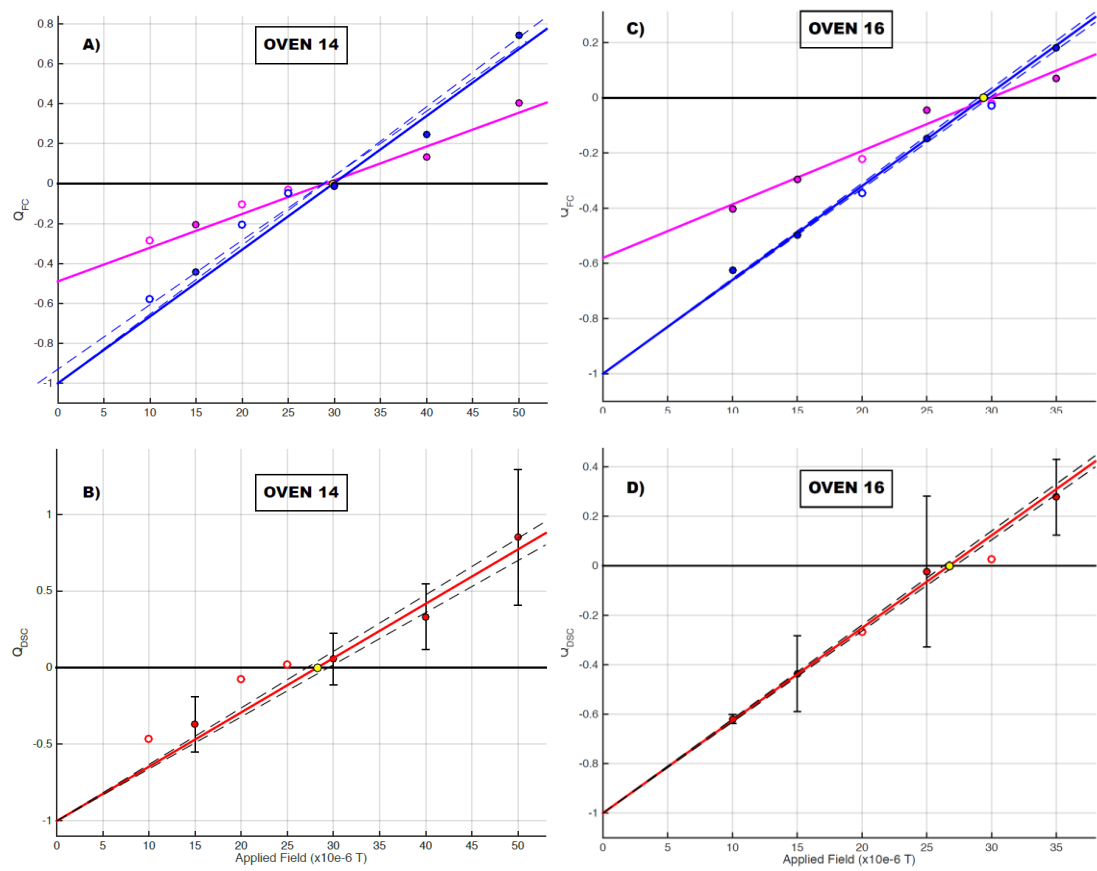
828

829   Fig. 7

830

831

a)

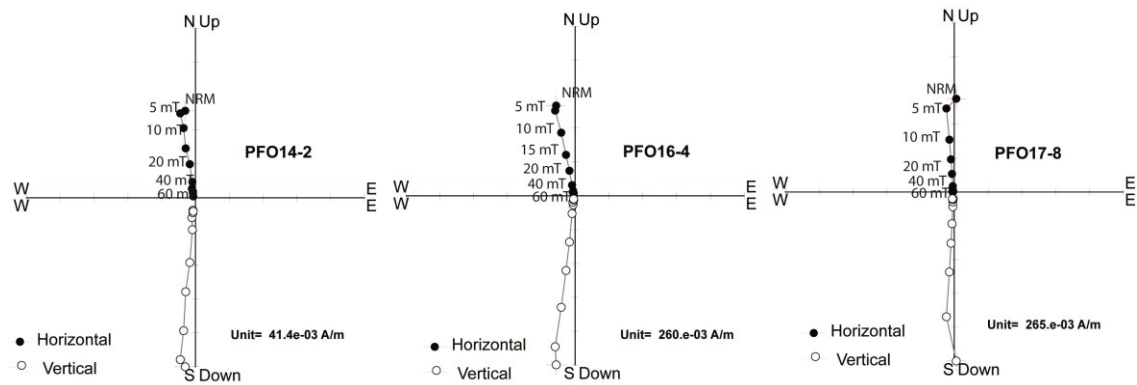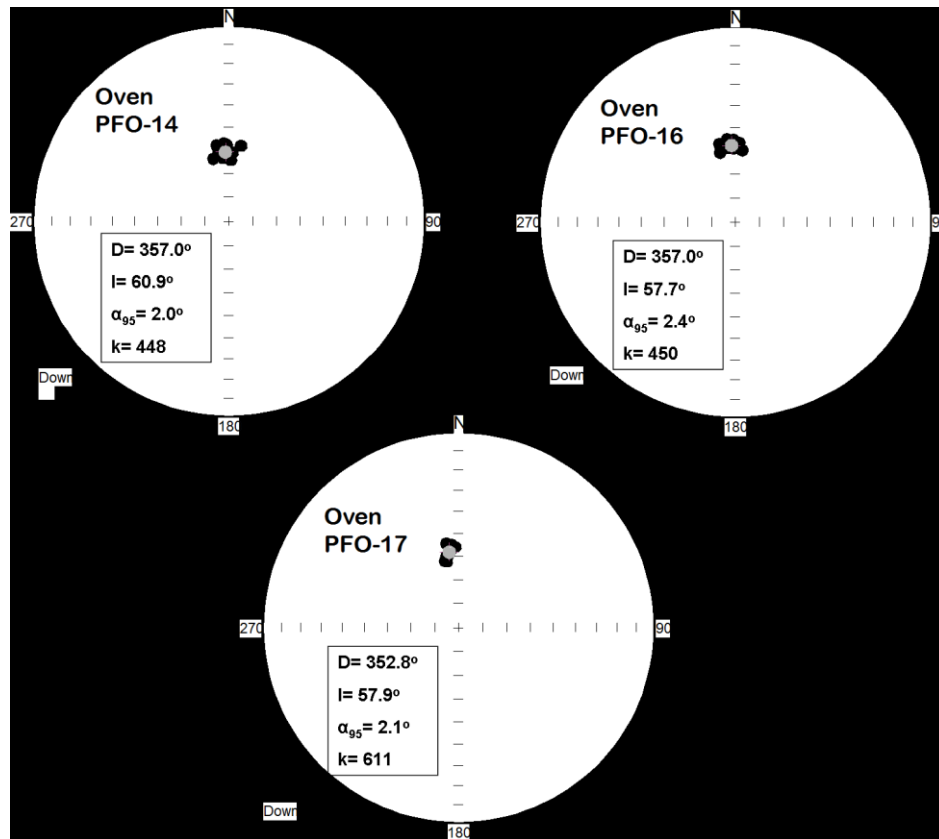b)

c)
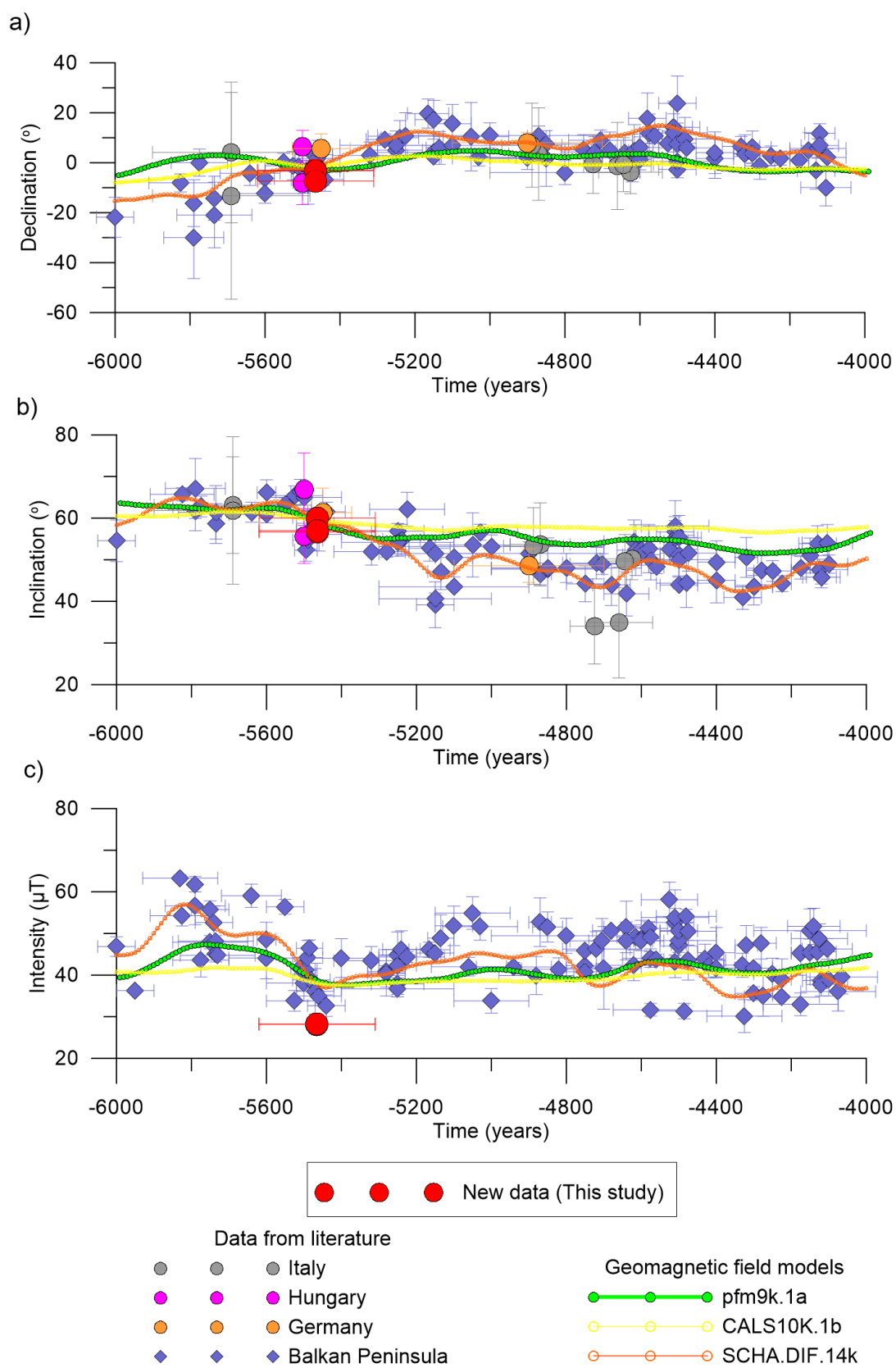
Fig. 8

835

836

837

838

		Bulk susceptibility				
Sample	NRM (E-03 A/m)	(E-03 SI)	P_{AMS}	D (º)	I(º)	MAD
Oven PFO14						
PFO14-1	526.9	4.253	1.011	358.5	57.8	1.3
PFO14-2	233.4	1.681	1.006	351.0	61.4	1.4
PFO14-3	377.0	2.848	1.009	9.3	57.7	0.9
PFO14-4	593.8	4.770	1.002	358.6	61.3	1.4
PFO14-5	351.6	2.548	1.012	354.9	63.4	1.4
PFO14-6	563.3	4.316	1.002	356.1	60.6	1.6
PFO14-7	869.9	5.898	1.011	355.0	61.5	1.3
PFO14-8	456.2	3.973	1.011	346.1	63.0	1.3
PFO14-9	509.8	4.173	1.007	356.4	57.0	2.4
PFO14-12	681.1	4.137	1.008	3.2	61.0	3.5
PFO14-13	705.7	4.648	1.007	2.1	64.3	1.8
PFO14-14	476.3	4.679	1.011	350.9	57.7	1.5
PFO14-15	567.8	4.368	1.006	357.9	63.4	1.6

Mean direction:

N= 13   **D$_m$= 357.0º**   **I$_m$= 60.9º**   **α$_{95}$= 2.0º**   **k=448**

Oven PFO16

PFO16-4	1479	7.090	1.007	347.7	60.1	0.7
PFO16-5	1438	6.271	1.007	2.8	56.4	0.9
PFO16-6	751.6	5.539	1.003	5.6	59.5	1.2
PFO16-7	1212	7.036	1.004	354.3	54.8	0.9
PFO16-8	899.2	5.725	1.013	354.8	58.7	1.3
PFO16-9	1022	5.516	1.007	1.7	57.7	1.4
PFO16-11	1399	7.888	1.007	358.9	59.0	1.1
PFO16-12	1223	7.030	1.010	358.8	55.2	1.5
PFO16-13	1110	6.848	1.008	348.4	56.3	1.3

Mean direction:

N=9   **D$_m$= 357.0º**   **I$_m$= 57.7º**   **α$_{95}$= 2.4º**   **k=450**

Oven PFO17

PFO17-7	916.78	9.441	1.003	351.2	59.5	1.9
PFO17-8	1514	10.94	1.002	355.4	55.1	1.4

PFO17-9	2043	12.39	1.023	357.7	56.0	1.0
PFO17-11	2143	10.65	1.004	353.5	57.7	0.9
PFO17-12	1753	10.13	1.002	356.1	56.0	1.3
PFO17-13	2100	13.14	1.004	349.8	61.8	0.9
PFO17-14	2089	14.96	1.003	348.3	61.4	1.4
PFO17-15	1985	11.94	1.005	350.2	59.6	0.9
PFO17-16	2287	12.57	1.003	351.8	54.0	2.5

Mean direction:

N=9   **D_m= 352.8º**   **I_m= 57.9º**   **α_{95}= 2.1º**   **k=611**

Table 1

Method	PI (µT)	65% conf.	n/N	R-squared	RMSE
Oven 14					
MSP-DB	29.0	[26.6 - 31.1]	4/7	0.9665	0.0575
MSP-FC	29.9	[28.9 - 30.9]	4/7	0.9766	0.0760
MSP-DSC (α = 0.2)	29.4	[27.1 - 29.4]	4/7	0.9701	0.1845
MSP-DSC (α = 0.8)	27.2	[28.3 - 30.6]	4/7	0.9546	0.1866
MSP-DSC (α = 0.5)	**28.2**	**[27.1 - 29.4]**	**4/7**	**0.9630**	**0.1842**
Oven 16					
MSP-DB	29.9	[28.3 - 31.9]	4/7	0.9746	0.0425
MSP-FC	29.4	[29.0 - 29.8]	4/7	0.9968	0.0205
MSP-DSC (α = 0.2)	27.8	[27.2 - 28.4]	4/7	0.9942	0.1076
MSP-DSC (α = 0.8)	25.7	[25.2 - 26.2]	4/7	0.9957	0.0860
MSP-DSC (α = 0.5)	**26.7**	**[26.3 - 27.2]**	**4/7**	**0.9972**	**0.0711**
Oven 17					
MSP	n.d.	n.d	3/7	n.d	n.d

Table 2